Journal of Mines, Metals and Fuels, *71(9): 1205-1214; 2023. DOI: 10.18311/jmmf/2023/35437*

Print ISSN : 0022-2755

Journal of Mines, Metals and Fuels

**Contents available at:** *www.informaticsjournals.com/index.php/jmmf*

# Effect of Scanning Strategy on Surface Roughness of Directed Energy Deposited Inconel 718 Alloy

**Ajay Kumar Maurya[1], Amit Kumar[1], Surendra Kumar Saini[2] and Ravi Kumar Gupta[3,4]***

*[1]Mechanical Engineering Department, National Institute of Technology Patna – 800005, Bihar, India*
*[2]Mechanical Engineering Department, Poornima College of Engineering Jaipur – 302022, Rajasthan, India*
*[3]Department of Mechanical Engineering, SAMM, Faculty of Engineering, Manipal University Jaipur, Jaipur – 303007, India;*
*[4]Department of Mechanical Engineering Education, National Institute of Technical Teachers' Training and Research, Bhopal - 462 002, India; rkgiisc@gmail.com*

## Abstract

*The additive manufacturing method based on powder feed type laser Directed Energy Deposition (DED) is projected to be able to create objects with intricate structures. The intricate thermal history that occurs during DED causes variations in the top surface roughness, which is an important quality index for DED and has a significant impact on the lifespan of the samples. Surface quality is always desirable, mostly in the case of dynamic loading applications. This article presents a methodical investigation into the top surface roughness of the Inconel 718 alloy during various scanning strategies in the DED. This alloy is utilized extensively in the aerospace, automotive, and military industries. Multilayer cuboid samples are fabricated using four scanning strategies. Using different scan strategy, no significant changes in pore size and amount of porosity was observed, but significant changes were observed for the surface quality of printed Inconel alloy.*

**Keywords:** *Additive Manufacturing, Directed Energy Deposition, Inconel 718, Surface Roughness*

## 1.0 Introduction

The term Additive Manufacturing (AM) refers to a set of manufacturing techniques that is quickly expanding, and there is a significant amount of research activity committed to further improving its potential. The process involves several processes, the first of which involves mixing the powder with carrier gases, which carry powders to the target plate through a nozzle, and the second involves sintering chosen areas of the substrate by raster scanning with a laser. This procedure results in the creation of a component that is encased in a loose powder, which is then extracted and recycled after the component has been completed. The development and application of AM have formally gotten underway. However, even though the velocity of this growth and the amount of innovation promise a bright future, there is still a great deal of hurdles to be overcome. Surface roughness and porosity are the major problems in the AM components. The roughness is mostly affecting the lifespan of dynamic loading components and fails before the expected service. So, it is essential to minimize and yet is a challenging task, in powder feed Laser Directed Energy Deposition (LDED) system[1].

The rate of energy supplied per unit volume of powder material is just one of several variables that might affect the outcome of a laser-directed energy deposition process. Because powder material melts differently depending on its qualities, it is crucial to apply precise process settings to optimize part quality. Due to this, more research into the LDED consolidation process is needed to determine when the laser heats the powder, especially the first layer

*Author for correspondence

on the platform, and how the process parameters are affecting the process. The literature review of the present study is revealed in Section 2. Experimental procedures and methods are mentioned in Section 3. The results of macro defects and porosity analysis of these components are presented in Section 4.1, whereas the surface topography is presented in Section 4.2.

## 2.0 Literature Review

One of the major criticisms of AM is that the finished product typically has an undesirable surface texture (roughness and waviness), often known as surface finish. An increase in surface texture can harm performance by increasing fluid friction factors associated with flow channels leading to higher pressure drops, mechanical friction and wear and corrosion potential in hostile conditions[2-4]. The laser-directed energy deposition method has been used to study surface roughness in a wide variety of metal alloys for thin-wall structures for several industrial purposes[5-7].

Implementing cladding deposition strategy, a study by Mahamood *et al.* on laser powder-directed energy deposition of Ti–6Al–4V showed that increasing laser power with a 2 mm spot size made the surface smoother[8]. Increasing the laser power increase, the powder melting, and less unmelted powder stick to the walls. However, the increase in power will change the shape of the walls. Kim *et al.* talk about how increasing the laser power and powder mass flow rate will make the layer width bigger and give a more uniform bead with fewer holes[9]. Increasing the laser power, a lot just for making thin structures is not a good way to build, since this leads to uncontrolled geometry.

Mazzarisi *et al.* deposited an Inconel 718 wall with a thickness of 1.5 mm. They found that increasing the laser power by 150% made the melt pool grow, which led to a 44% increase in wall thickness[10]. Jinoop *et al.* printed nickel alloy with LDED and found that laser power had the most effect on the deposition geometry (width, height, and deposition rate), while powder feed rate and travel speed had less effect on the deposition geometry. It is also important that how these deposition parameters work together since changing them one at a time might not always get the desired result[11]. Zhang *et al.* evolved an optimal solution for building orientation during additive manufacturing using multi-attribute decision-making techniques[12]. Giganto *et al.* manufactured 17-4PH parts considering hexagonal, concentric, and normal scanning strategies to optimize the Selective Laser Melting process. They made conclusions that the hexagonal strategy was most appropriate in terms of porosity. Both normal and hexagonal strategies have good geometrical and dimensional quality[13]. Keles *et al.* evaluated the wetting feature of three-dimensional fabricated titanium alloy with an angle contact method. They reported that the fabricated surface varied the wetting state of a surface due to texture topology[14]. The build orientation of direct metal laser sintered fabricated Inconel alloy. They investigated the microstructural characteristics of the built part. It was revealed that surface roughness relies on build orientation and scan strategy, but density not depend on scan strategy[15,16]. Hashmi *et al.* reported the formation of surface defects during additive manufactured metallic parts at lower laser power, but with higher laser power the surface defect minimizes[17]. It is found in the literature that surface properties of parts printed using different additive manufacturing techniques and changing process parameters have different surface quality, so the surface quality depends on technique and process parameters used.

According to the literature, the primary issues with the LDED process are surface roughness and geometric errors. These problems can be controlled by a better understanding of how the process works. A few studies evaluate the surface roughness using the LDED process but are limited in the application of thin-wall structure. In this study, the effect of the scanning strategy on the top surface roughness and porosity of bulk structure are investigated.

## 3.0 Experimental Procedure and Methods

Inconel 718 powder is used in the experiments. Powder size is measured using the SEM image with the aid of ImageJ software. Typically, powder particle size varies between 30-120 µm in the LDED process [11]. In the present study, the measured range of powder particle size is in the range of 40–110 µm with the maximum particle size range of 70–80 µm. The particle size distribution is shown in Figure 1. It clearly shows that Inconel 718 powder size is highly qualified for printing with the LDED process. The chemical composition of the powder is given in Table 1.

**Table 1.** Chemical composition of used Inconel 718

| Element | Ni | Cr | Nb | Mo | Ti | Al | Co | Cu | C | B | Fe |
|---|---|---|---|---|---|---|---|---|---|---|---|
| Weight (%) | 50-55 | 17-21 | 4.75-5.5 | 2.8-3.3 | 0.65-1.15 | 0.2-0.8 | ≤1 | ≤0.3 | ≤0.08 | ≤0.006 | Balance |

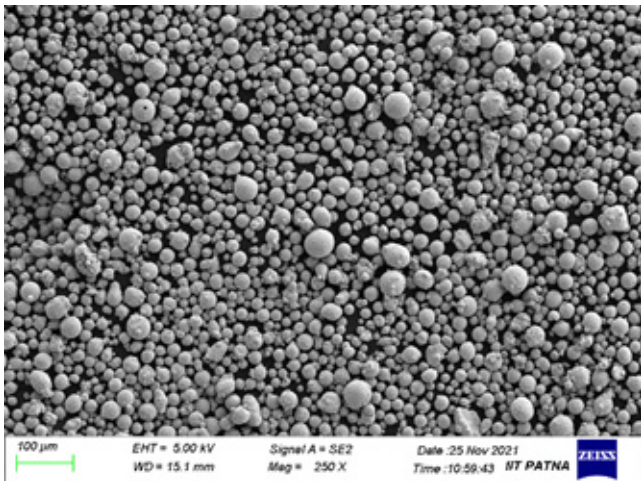


**Figure 1.** Powder morphology of Inconel 718 alloy.

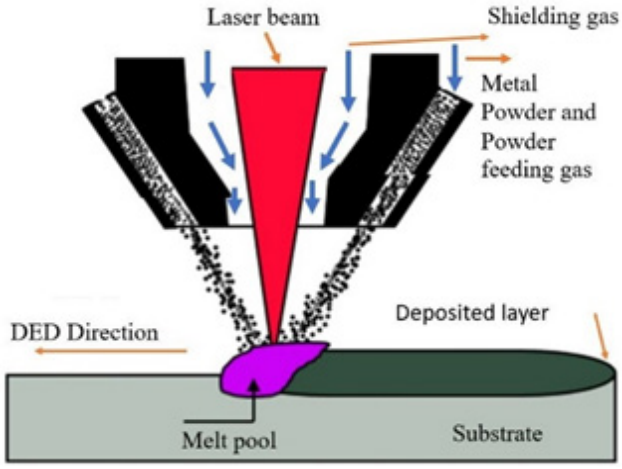


**Figure 2.** Directed energy deposition process.

The experiments were conducted on an indigenously developed LDED system. Figure 2 presents the schematic of the LDED process. This system consists of a fibre laser of 2 kW laser capacity and a twin powder feeder system. Carrier gases carry the powder particles and supply them to the target plate during the process. The system uses a 5-axis workstation placed inside a controlled atmosphere chamber (glove box). However, in the present work, three axes, i.e., X, Y, and Z, are only used for experiments. The glove box with an appropriate gas feeding system facilitates the usage of inert gas to provide an inert atmosphere for the LDED process. The glove box is provided with an antechamber for loading and unloading components and parts on the workstation during the processing without impeding the controlled atmosphere. Oxygen and moisture sensors have been installed in the system to provide information about the current level of oxygen and moisture content inside the glove box.

The LDED processing parameters and scanning strategy selected after trial experiments are given in Tables 2 and 3, respectively. The experiments are performed in the presence of an inert gas mixture (Argon + Helium). The commercially available stainless steel 316L substrate plate was used for material deposition. Thus, three-dimensional components (Inconel 718) of cuboid shape in a layer-by-layer fashion are fabricated accordingly to designed scan strategies as shown in Figure 3.

**Table 2.** Process parameters of structure deposition

| Parameter | Value |
|---|---|
| Laser power | 1050 W |
| Scan speed | 0.6 m/min |
| Powder feed rate | 9 g/min |
| Hatch scaping | 2 mm |
| Overlap | 50% |

The scan directions for the first four layers are presented in Table 3 which are then followed to build the remaining solid. Many experiments were conducted with different scanning strategies to analyse the effect on the surface roughness. Four scan strategies are selected to show the effect on the surface roughness of the manufactured components. The selected scan strategies have distinct combinations of the track's angle, layer's angle, and laser scan direction. The laser scan directions

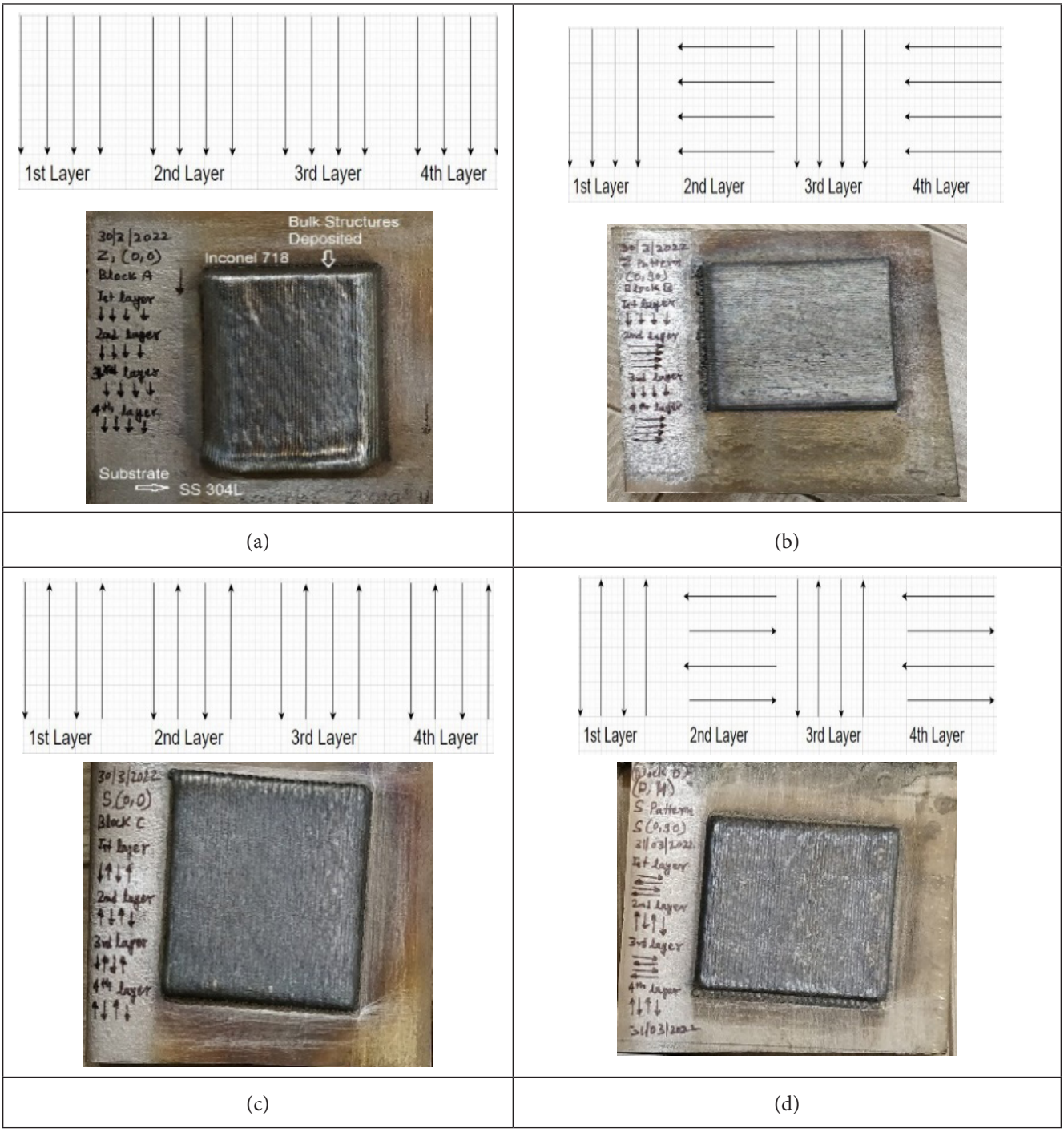


**Figure 3.** LDED printed Inconel 718 bulk structures (cuboid shape) on SS 316L at different scan strategies.

can be different within a layer and between the layers. The results of the study are presented in the following section.

The LDED used four different scanning procedures to build the Inconel 718 samples of the cuboid shape of 50 mm, 50 mm, and 10 mm sides. The laser beam moves as per the selected four designed scanning strategies as presented in Table 3. Scanning strategy, A: as can be seen in Figure 3 (a), the laser beam follows a linear pattern

**Table 3.** Different scan patterns strategies for depositing different bulk structures

| Scan strategy | Track's angle ($\theta_T$) | Layer's angle ($\theta_L$) | 1st layer | 2nd Layer | 3rd layer | 4th layer |
|---|---|---|---|---|---|---|
| A | 0 | 0 | ↓↓↓↓ | ↓↓↓↓ | ↓↓↓↓ | ↓↓↓↓ |
| B | 0 | 90 | ↓↓↓↓ | ↑↑↑↑ | ↓↓↓↓ | ↑↑↑↑ |
| C | 180 | 0 | ↓↑↓↑ | ↓↑↓↑ | ↓↑↓↑ | ↓↑↓↑ |
| D | 180 | 90 | ↓↑↓↑ | ↓↑↓↑ | ↓↑↓↑ | ↓↑↓↑ |

that is perfectly horizontal across each track, and each new layer is parallel to the previous layer. There is no inclination at all. Scanning strategy B: as shown in Figure 3 (b), the laser beam makes a linear (horizontal) pattern with the previous track to make a layer, but each new layer makes an angle of 90 degrees with the subsequent layer. Scanning strategy C: as shown in Figure 3 (c), the path that the laser beam follows in each track is linear, but the subsequent track makes an angle of 180 degrees. In this strategy, each new layer is parallel to the previous layer as the angle between the two layers is 0 degrees. Figure 3 (d) shows a scanning technique referred to as D, in which the laser beam moves linearly with an angle of 180 to 0 degrees for each alternating track that makes a layer. Here, the alternating layer makes an angle of 90 degrees with the previous layer. The printed samples of work material are shown in Figure 3.

## 4.0 Results and Discussion

These manufactured samples were examined for surface porosity and surface roughness. The samples were cut into cubic shapes of 10 mm side on a wire-EDM and then polished and sealed with resin for porosity analysis. Optical microscopy was used to get photos. Images of the polished surfaces of the samples were combined and analysed in ImageJ software to determine the level of porosity. The results of macro defects and porosity analysis of these components are presented in Section 4.1. The surface roughness of samples was measured using an optical profilometer. The LDED-made components' uneven surface quality necessitated five measurements taken in a variety of directions across the top surface and the calculations of arithmetic mean roughness (Ra) were made. The surface topography is presented in Section 4.2. Samples made using each of the four scanning methods

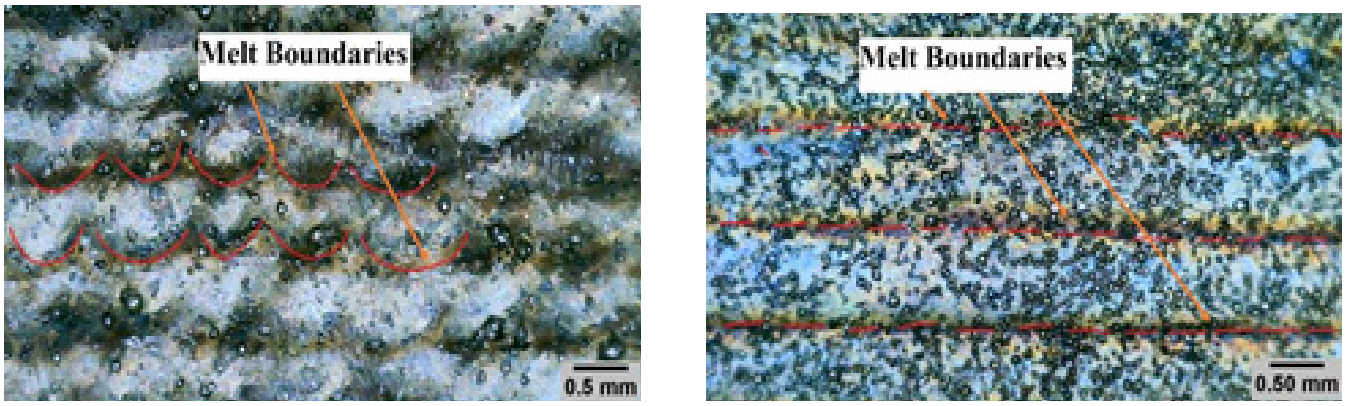


(a) (b)

**Figure 4.** Melt-pool boundaries along (a) Cross-section, and (b) Top surface.

were analysed for porosity and surface quality to decide which scan strategies would be best for the intended use of the finished product.

## 4.1 Macro Defects and Porosity Analysis

Macro-scale melt-pool analysis along the cross-section and top surface of the deposit is presented in Figures 4 (a) and (b), respectively. Overlapping melt pools are visible along the deposit's cross-section and top surface. The melt-pool borders can be seen as almost defect-free. Additionally, optical microscopy is used to examine the very small defects in the LDED-built Inconel 718 bulk structure.

The porosity of the analyzed samples is shown in Figure 5. It is observed that the samples created by LDED are rarely found with microcracks whereas micro-pores are seen. At isolated locations, few visible pores are seen as (i) mixture of gases referred to as gas porosity and (ii) process-induced porosity due to lack of fusion. Gas porosity (indicated by continuous circles in Figure 5) is caused by either porosity within the powder because of the powder manufacturing process or gas trapped within the melt pool during the solidification. Process-induced porosity (marked with dotted lines in Figure 5) might be a result of inadequate material melting in specific regions[18].

The area fraction technique is used to estimate the relative porosity of the surface, which have a size of almost 10 to 20 microns. The porosity for different cubic structures that are built using different scanning strategies is given in Table 4. Observing Table 4, it was found that the cube fabricated using scan strategy D has a relatively lower porosity than other strategies. The D strategy exhibits lower percentages of exterior and open porosity as compared to the other three strategies. The D method yields the best results in terms of the overall porosity of the samples. But, the porosity differences between different scanning strategy very low.

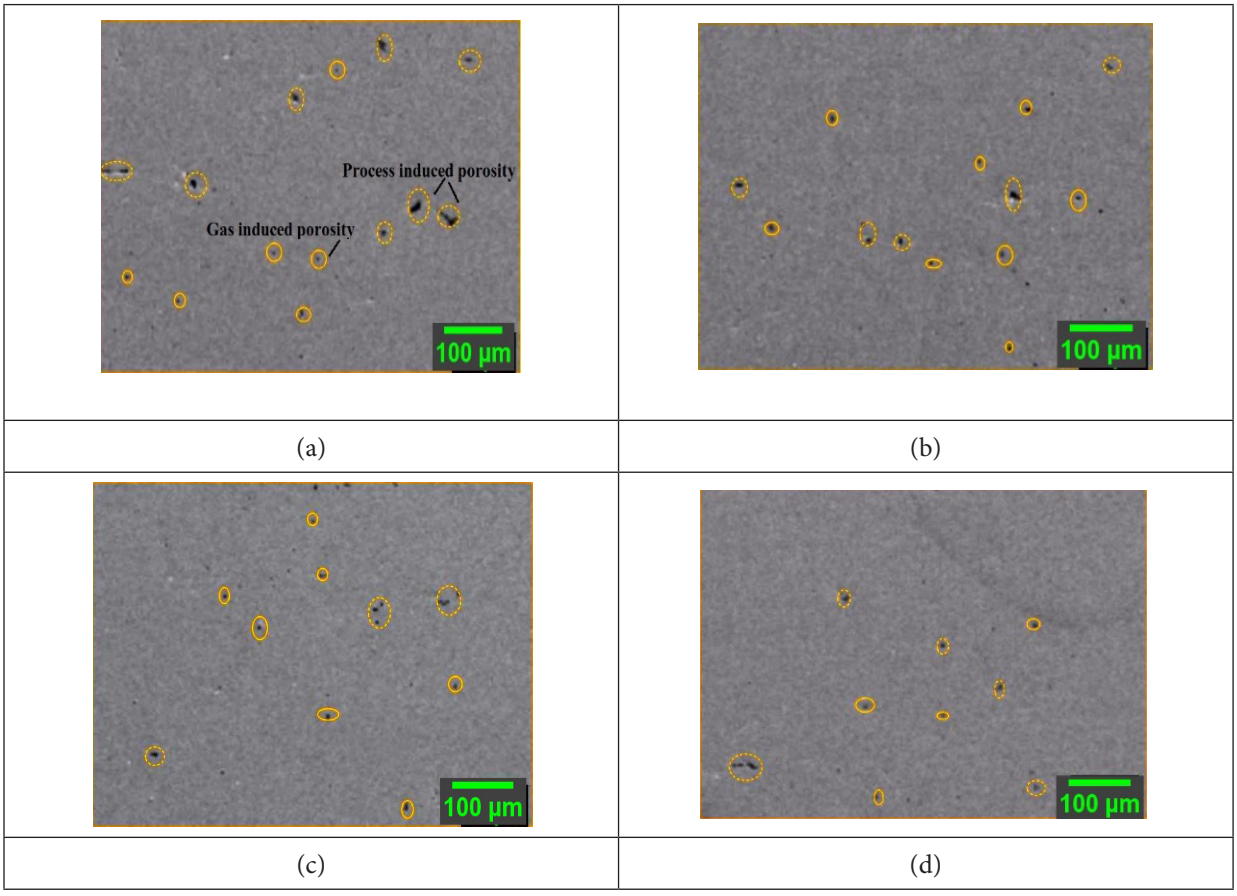


**Figure 5.** Porosity analysis of LDED-built cube structures on the top surface at different scan strategies (a) A, (b) B, (c) C, and (d) D.

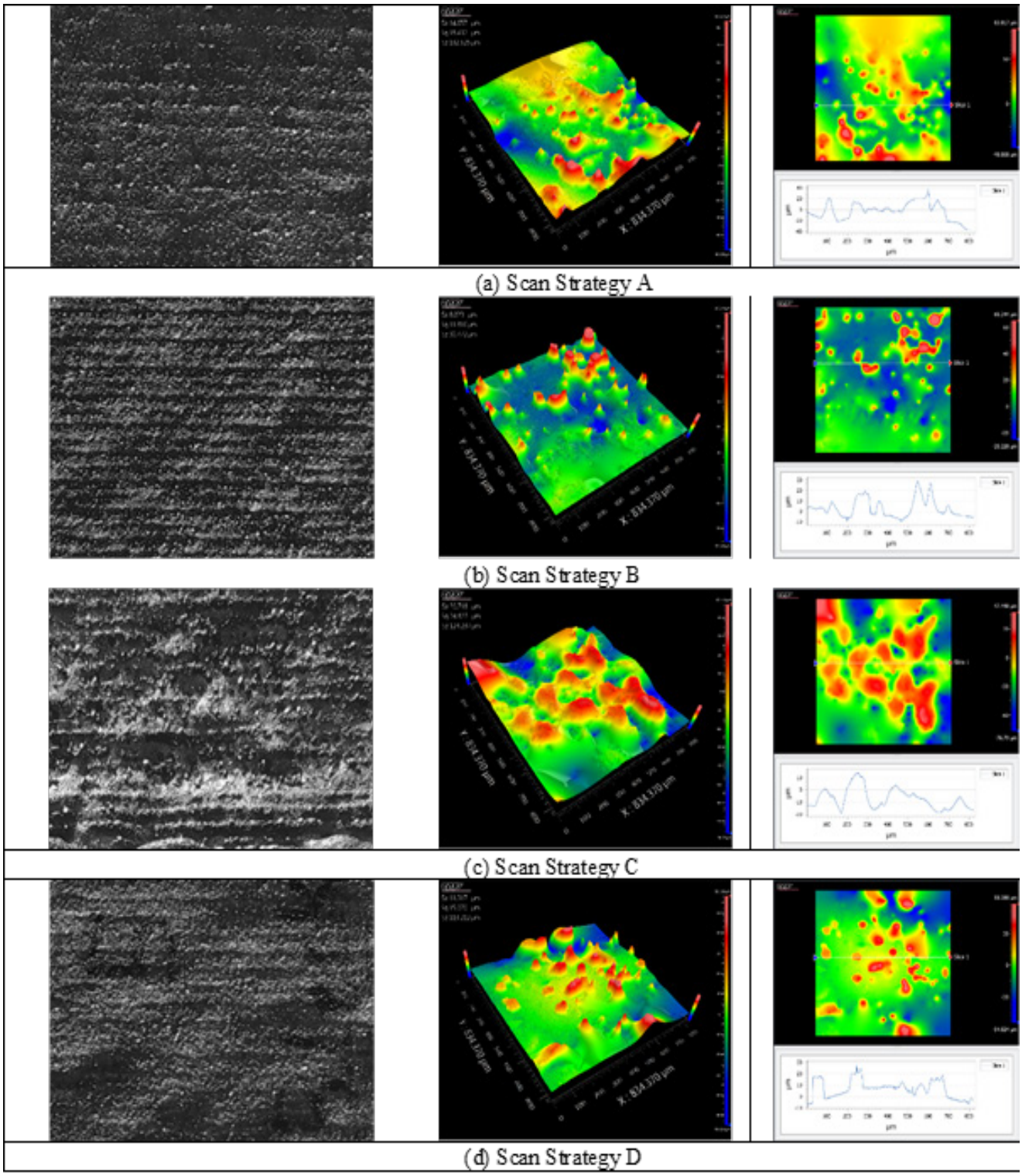


**Figure 6.** Images (a), (b), (c), and (d) represent different bulk structures' top surface topography and roughness of samples fabricated using different scan strategies A, B, C, and D, respectively. (The first column shows stereo microscopy images, the middle column optical profilometer microscopy images, and the third column surface roughness images).

It is observed in Table 4 that the scan strategy did not have much impact on pore size and pore concentration, but different scan strategies had different distributions of void circularity and area. This finding suggests that the scan approach influences the type of defects created but not the absolute concentration of voids/pores. Although overlap in the material can result in re-melting, which creates a uniform but alternating microstructure, the scanning strategy affects the cooling time, which affects the final grain structure.

**Table 4.** The porosity % of LDED built structures at various scan strategies

| Scan strategy | porosity % |
|---|---|
| A | ~0.53±0.1 |
| B | ~0.51±0.1 |
| C | ~0.45±0.1 |
| D | ~0.42±0.1 |

## 4.2 Surface Topography Analysis

The surface topography of the LDED-built Inconel 718 cubic structures is analyzed in as-built condition using microscopy and an optical profilometer. The surface topography for the Inconel 718 cube made using the four scanning strategies is shown in Figure 6, where the first column shows stereo microscopy images, middle column optical profilometer microscopy images, and third column surface roughness images. The presence of partially melted powders and stack a layered pattern can be seen on the surface of printed samples. The


**Figure 7.** Surface roughness of different structures at different scan strategies.

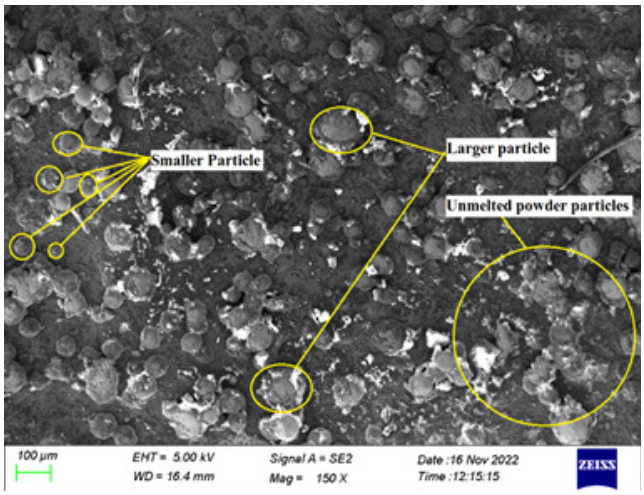


**Figure 8.** Microscopic image of the top surface of LDED printed Inconel 718.

observed pattern on the surface of the built structure is due to the overlapped laser scans during deposition. The distance between the two lines is in the range of 1.20 mm to 1.35 mm, which is equal to the hatch spacing used during the LDED process. The stack layer pattern during the deposition contributes to the waviness of the built surface. The roughness is mainly governed by the presence of powders that have partially melted and are present on the deposit's surface. The primary causes of partially melted powders are scattering due to higher laser energy deposition, lack of 100% powder catchment during deposition, and powder particle size and shape.

The findings of the roughness study indicate that the measured surface as well as the scanning method have an impact on the final surface of the built samples. The top surface of the sample built using scan strategy B has the lowest roughness values, while the sample built using scan strategy C has a higher roughness value as presented in Figure 7. In comparison to scan strategy C, both the A and D strategies include a more manageable level of roughness. On the other side, there is a discernible decline seen in the samples produced using the B strategy, with the value of Ra 8.2 µm reaching its lowest point ever. In addition, surface roughness measures look like what is shown in Figure 7. The roughness is found in the range of 8 µm to 12 µm. It is found that the cross-deposited structure has a relatively lower surface roughness than the unidirectional deposits. It is found that scan strategy B, relatively, has lower surface roughness due to uniform layer deposition, which produces a uniform surface. It

is possible to conclude from these data that the B laser trajectory results in the best surface finish when applied to the top surfaces. These findings are in agreement with the low levels of exterior porosity as seen in the B samples (Figure 5). Finally, the varying surface roughness occurs due to changing the specific area of heat flow which is different in different scanning strategy results in different unmelted powder particles and varying surface roughness.

The surface roughness is the unmelted powder particle present on the surface. Here in Figure 8, it can be seen that unmelted powder particles present on the surface play an important role in surface quality. Lack of laser power or lack of specific energy results in unmelted powder particles on the surface. Changing the scanning strategy produces varying specific energy in different regions, which produces different numbers of unmelted particles. The unmelted powder particles may be less or more depending upon the availability of energy. The unmelted powder particle is responsible for surface roughness. As the powder particle size increases, the roughness of the surface also increases which is validated by the macroscopic picture of the surface at a higher magnification shown in Figure 8.

## 5.0 Conclusion

The work presented the laser-directed energy deposition technique to print the Inconel 718. Four scanning strategies were used to fabricate the sample of the cuboid shape of 50 mm, 50 mm, and 10 mm sides made of Inconel 718. Porosity and surface quality of printed material analysed. Following are the findings that have been reached to pick the LDED manufacturing scanning approach.

- Sample with scan strategy D is acceptable in terms of porosity due to the properties of its pores (size and shape), as well as the fact that it exhibits the lowest percentage of open and external pores. But comparing with the other scanning strategy no statistically significant differences were observed between them, which concludes that the scanning strategy has no major impact on pore size.
- Discernible variations are seen between the surface finishes of the samples printed with different scanning strategies, i.e., A, B, C, and D. The variation in the surface roughness occurs due to changes in the specific area of heat flow, which occurs due to the scanning strategy responsible for different unmelted powder particles on the surface which produces varying surface roughness.
- The surface roughness of fabricated Inconel 718 is found minimum at the track angle and layer angle of zero and 90 degrees, respectively. The sample with scan strategy B is found lowest roughness followed by the sample with scan strategy D, A, and C. However, LDED printed parts need post-processing to enhance the surface quality.

## 6.0 Acknowledgment

Thanks to all staff of RRCAT, Indore and NIT, Patna, for providing their experimental facilities.

## 7.0 References

1. Bahnini I, Rivette M, Rechia A, Siadat A, Elmesbahi A. Additive manufacturing technology: The status, applications, and prospects. The International Journal of Advanced Manufacturing Technology. 2018; 97:147–61. https://doi.org/10.1007/s00170-018-1932-y
2. Khan HM, Karabulut Y, Kitay O, Kaynak Y, Jawahir IS. Influence of the post-processing operations on surface integrity of metal components produced by laser powder bed fusion additive manufacturing: A review. Machining Science and Technology. 2020; 25:118–76. https://doi.org/10.1080/10910344.2020.1855649
3. Stimpson CK, Snyder JC, Thole KA, Mongillo D. Scaling roughness effects on pressure loss and heat transfer of additively manufactured channels. Journal of Turbomachinery; 139(2). https://doi.org/10.1115/1.4034555
4. Hemmasian Ettefagh A, Guo S, Raush J. Corrosion performance of additively manufactured stainless steel parts: A review. Additive Manufacturing. 2021; 37. https://doi.org/10.1016/j.addma.2020.101689
5. Wu Z, Narra SP, Rollett A. Exploring the fabrication limits of thin-wall structures in a laser powder bed fusion process. The International Journal of Advanced Manufacturing Technology. 2020; 110:191–207. https://doi.org/10.1007/s00170-020-05827-4
6. Fox JC, Moylan SP, Lane BM. Effect of process parameters on the surface roughness of overhanging structures in laser powder bed fusion additive manufacturing.

Procedia CIRP. 2016; 45:131–4. https://doi.org/10.1016/j.procir.2016.02.347
7. Jamshidinia M, Kovacevic R. The influence of heat accumulation on the surface roughness in powder-bed additive manufacturing. Surface Topography: Metrology and Properties. 2015; 3(1). https://doi.org/10.1088/2051-672X/3/1/014003
8. Mahamood RM, Akinlabi ET. Effect of Powder Flow Rate on Surface Finish in Laser Additive Manufacturing Process. IOP Conference Series: Materials Science and Engineering, Volume 391, The 1st International Conference on Engineering for Sustainable World (ICESW) 3–7 July 2017, Ota, Nigeria; 2018. https://doi.org/10.1088/1757-899X/391/1/012005
9. Kim MJ, Saldana C. Thin wall deposition of IN625 using directed energy deposition. Journal of Manufacturing Processes. 2020; 56:1366–73. https://doi.org/10.1016/j.jmapro.2020.04.032
10. Mazzarisi M, Campanelli SL, Angelastro A, et al. Phenomenological modelling of direct laser metal deposition for single tracks. The International Journal of Advanced Manufacturing Technology. 2020; 111:1955–70. https://doi.org/10.1007/s00170-020-06204-x
11. Jinoop AN, Paul CP, Denny J, et al. Laser additive manufacturing (LAM) of Hastelloy-X thin walls using directed energy deposition (DED): Parametric investigation and multi-objective analysis. Lasers in Engineering. 2020; 46:15-34.
12. Zhang Y, Wu L, Guo X, Kane S, Deng Y, Jung Y-G, *et al*. Additive manufacturing of metallic materials: A review. Journal of Materials Engineering and Performance. 2017; 27:1–13. https://doi.org/10.1007/s11665-017-2747-y
13. Giganto S, Martínez-Pellitero S, Barreiro J, Leo P, Castro-Sastre MA. Impact of the laser scanning strategy on the quality of 17-4PH stainless steel parts manufactured by selective laser melting. Journal of Materials Research and Technology. 2022; 20:2734–47. https://doi.org/10.1016/j.jmrt.2022.08.040
14. Keles O, Qadeer A, Yilbas BS. Wetting state of 3D printed Ti-6Al-4V alloy surface. Advances in Materials and Processing Technologies. 2022; 8:2465–75. https://doi.org/10.1080/2374068X.2021.1912539
15. Maurya AK, Kumar A. The influence of building direction and conventional heat treatment on the microstructure, physical, and mechanical characteristics of direct metal laser sintered Inconel 718 alloy. Advances in Materials and Processing Technologies. 2022. https://doi.org/10.1080/2374068X.2022.2081296
16. Maurya AK, Kumar A, Saini SK, Paul CP. Optimization of track height of LDED inconel Alloy-718. Nano World Journal. 2023; 9(S1):S188–9. https://doi.org/10.17756/nwj.2023-s1-038
17. Hashmi AW, Mali HS, Meena A, Puerta APV, Kunkel ME. Surface characteristics improvement methods for metal additively manufactured parts: A review. Advances in Materials and Processing Technologies. 2022; 8:4524–63. https://doi.org/10.1080/2374068X.2022.2077535
18. Slotwinski JA, Garboczi EJ. Porosity of additive manufacturing parts for process monitoring. AIP Conference Proceedings. 2014; 1581:1197–204. https://doi.org/10.1063/1.4864957